ACS APPLIED MATERIALS & INTERFACES

Research Article

www.acsami.org

Vapor Phase Polymerization Deposition of Conducting Polymer/Graphene Nanocomposites as High Performance Electrode Materials

Yajie Yang, Shibin Li,* Luning Zhang, Jianhua Xu, Wenyao Yang, and Yadong Jiang

State Key Laboratory of Electronic Thin Films and Integrated Devices, School of Optoelectronic Information, University of Electronic Science and Technology of China (UESTC), Chengdu 610054, P. R. China

ABSTRACT: In this paper, we report chemical vapor phase polymerization (VPP) deposition of novel poly(3,4-ethylenedioxythiophene) (PEDOT)/graphene nanocomposites as solid tantalum electrolyte capacitor cathode films. The PEDOT/graphene films were successfully prepared on porous tantalum pentoxide surface as cathode films through the VPP procedure. The results indicated that the high conductivity nature of PEDOT/graphene leads to the decrease of cathode films resistance and contact resistance between PEDOT/graphene and carbon paste. This nanocomposite cathode film based capacitor showed ultralow equivalent series resistance (ESR) ca. 12 mΩ and exhibited better capacitance-frequency performance than the PEDOT based capacitor. The leakage current investigation revealed that the device encapsulation process does not influence capacitor leakage current, indicating the excellent mechanical strength of PEDOT-graphene films. The graphene showed a distinct protection effect on the dielectric layer from possible mechanical damage. This high conductivity and mechanical strength graphene based conducting polymer nanocomposites indicated a promising application future for organic electrode materials.

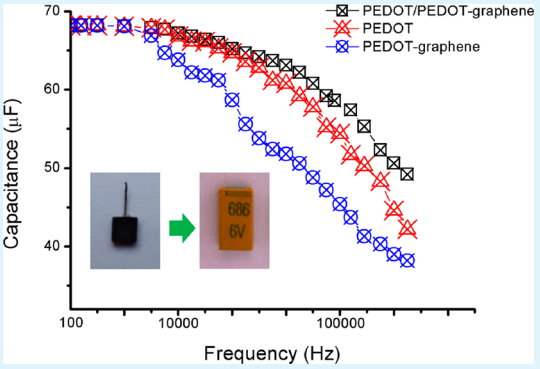

KEYWORDS: *vapor phase polymerization, conducting polymers, graphene, nanocomposites, solid tantalum electrolyte capacitor*

1. INTRODUCTION

In recent years, conducting polymers (CPs) and their nanostructures have been a subject of growing interest for their promising application in microelectronics, capacitors, sensors, solar cells, etc.[1−4] They offer a high conductive and optical transparent capability for electrode materials applied on capacitors and solar cells. The optimized device performance has been improved due to the construction of CPs and their nanostructures for electrode materials and modified electrode surfaces.[5−7]

As an important electronic device, the sintered tantalum powder structure makes solid tantalum electrolyte capacitors (STEC) volumetrically efficient, leading to compact porous construction and large capacitance. CPs, such as poly (3,4-ethylenedioxythiophene) (PEDOT), have been used as STEC cathode films owing to its higher conductivity and reliability, which produces high performance STEC with low equivalent series resistance (ESR).[8] However, PEDOT is brittle and weak in mechanical strength, and this is one of the drawbacks for the use of PEDOT as STEC electrodes. Coupling CPs with carbon nanomaterials has been demonstrated as an effective approach to improve the mechanical strength and conductive performance of the CPs, and it also shows a promising future for device applications.

It is a challenge to prepare electrode films by the use of uniform nanostructured CPs on special substrates, especially on a porous surface structure. The stiffness of their all-conjugated aromatic backbone structures is a hindrance for preparing electrode films.[9−13] The common process used to prepare cathode films on porous tantalum pentoxide is a solution based deposition process utilized to fabricate STEC. However, it is a challenge to use this deposition process due to the decrease of tantalum particle size causing larger capacitance with smaller size. As tantalum particle size decreases, it is difficult to prepare uniform CP films onto a micro/nano porous tantalum pentoxide structure surface by the use of the solution based deposition method.

Compared with other techniques used to obtain micro/nano structure CPs, vapor phase polymerization (VPP) has attracted attention because of its simplicity and controllability.[14,15] The VPP process is a facile way to prepare conducting polymer and nanocomposites on special substrate, such as porous structure substrate.[16] Polymer is synthesized by delivering monomers to a surface through the vapor phase, and it is solvent free. The VPP method is easily used to form well-defined chemical films directly on the different morphology surface or template. The oxidant plays the role of template, leading to particularly ordered polymers and sometimes crystalline ones. Such polymer nanostructures with significantly higher charge conductivities are formed. The conducting polymer nano-

Received: February 11, 2013
Accepted: April 26, 2013
Published: April 26, 2013

   dx.doi.org/10.1021/am4003815 | ACS Appl. Mater. Interfaces 2013, 5, 4350−4355

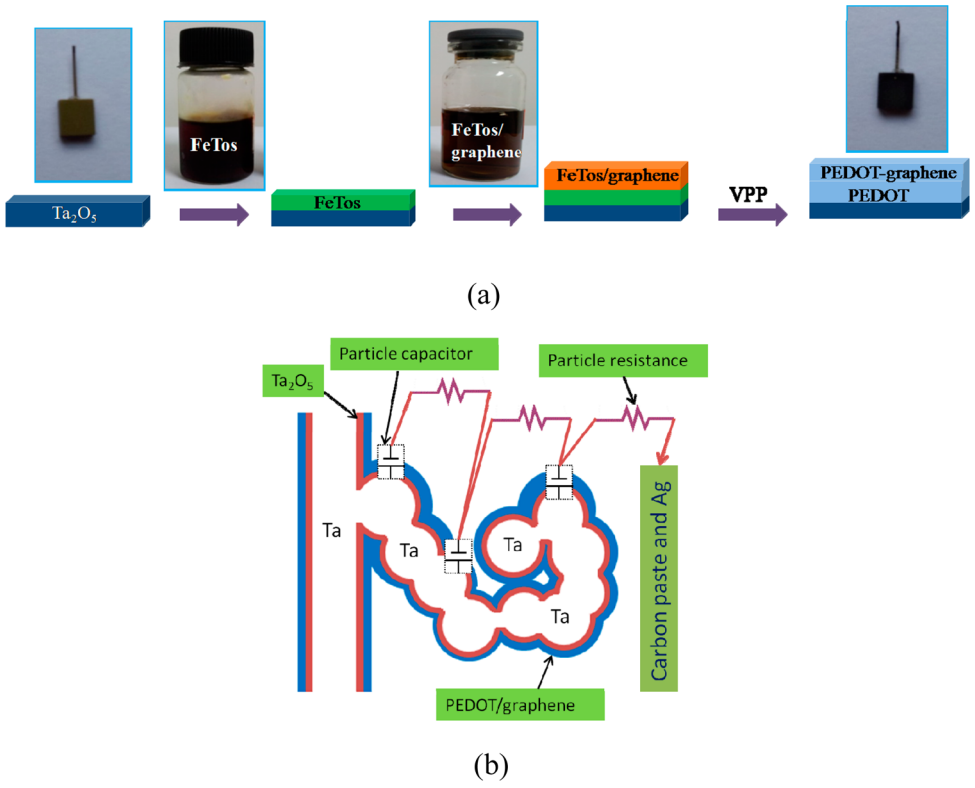

Figure 1. Schematic of (a) VPP deposition of PEDOT/PEDOT-graphene on Ta_2O_5 as cathode films and (b) structure of VPP film based capacitor.

composite with excellent electrical and thermal stability is suitable for high performance capacitor electrode materials. Moreover, the simple and controllable preparation method of VPP also makes the fabrication of high performance capacitors and nanocapacitors easy.[17,18] The VPP self-assembly deposition of PEDOT has been reported by some research teams, and this VPP conducting polymer film is a promising candidate to be used on solar cells and supercapacitors.[19−22]

In this work, VPP deposition of PEDOT and PEDOT-graphene on porous Ta_2O_5 is used as tantalum electrolyte capacitor cathode films. To the best of our knowledge, limited work is focused on fabricating PEDOT and PEDOT nanocomposites as SETC electrode films through the simple VPP process. In the first step, oxidant and oxidant-graphene nanocomposite for polymerization are successively prepared on the porous tantalum pentoxide surface by dip-coating. In the second step, the exposure of oxidant films on 3,4-ethylenedioxythiophene (EDOT) monomer gas is used to convert the oxidant/oxidant-graphene films into PEDOT/PEDOT-graphene composite films. The inner PEDOT layer constructed on Ta_2O_5 is for full capacitance extraction, and the outer PEDOT-graphene layer constructed on PEDOT improves conductive ability and mechanical strength of cathode films. The PEDOT and PEDOT/graphene film based electrolyte capacitor are constructed by this simple VPP procedure, and the electrical performance of capacitors was studied.

2. EXPERIMENTAL SECTION

Solutions of oxidant iron(III) *p*-toluenesulfonate (FeTos) (40 wt %) in butanol and 3,4-ethylenedioxythiophene (EDOT) were from HC Starck (under the respective trade names Clevios CB40 and Clevios M). Graphene dispersion and other reagents were purchased from Sigma-Aldrich and used without further purification. A porous tantalum sintering pellet (tantalum powder specific volume = 100 000 μf·V) for fabricating capacitor was purchased from Xinyun electronic company.

Ta powder was first pressed into regular bulk with size 3.2 mm × 2.4 mm × 2.8 mm to prepare porous anode. Then, these porous anodes were sintered at 1250 °C in a vacuum oven to remove impurity and obtain porous anodes with good mechanical behavior. After the sinter process, the Ta porous anodes were soaked in 2.5% phosphoric acid at 65 °C to form Ta_2O_5 dielectric. The formation voltage and current were 48 V and 15 mA/g, respectively. The Ta_2O_5 covered porous anode pellet was dipped into FeTos solution successively, and the FeTos solution was dip-coated onto the Ta_2O_5 surface. This process was carried out in a KSV dip-coating instrument with a 0.5 mm/min dipping speed, which ensures a well soaking process of oxidant solution into the porous Ta_2O_5 structure. Then, the FeTos covered anode body was put in a 60 °C vacuum oven for solvent evaporation. Oxidant layer was grown by a repeated dip-coating and drying process. After the preparation of inner FeTos layer, a FeTos/graphene outer layer was introduced on FeTos films by a dip-coating and drying process. The mass percentage of graphene in graphene/FeTos solution was 15% (wt %). The thickness of this outer layer increased by repeating the process. Following the construction of FeTos and FeTos/graphene films, the tantalum sintering pellet was transferred into a small vial full of EDOT monomer vapor. The FeTos and FeTos/graphene films were exposed on EDOT monomer vapor for 1 h to ensure complete polymerization. After the polymerization, the PEDOT/PEDOT-graphene films were then soaked in ethanol for 10−15 min and dried in a vacuum oven at 40 °C for 30 min. To complete tantalum capacitor construction, graphite and Ag pastes were deposited on PEDOT/graphene in sequence to form the electrical contact. The schematic VPP deposition and capacitor structure are shown in Figure 1.

UV−vis-NIR spectra were recorded with a UV1700 spectrophotometer (Shimadzu, Japan). The FT-IR spectrum was characterized with a WGH-30 analysis instrument (Tianjin, China). XRD patterns were recorded on Bruker AXS D8 at scanning speed of 0.02 °/s and an accelerating voltage of 40 kV. Film surface morphology was investigated with a Hitachi made scanning electron microscope

dx.doi.org/10.1021/am4003815 | ACS Appl. Mater. Interfaces 2013, 5, 4350−4355

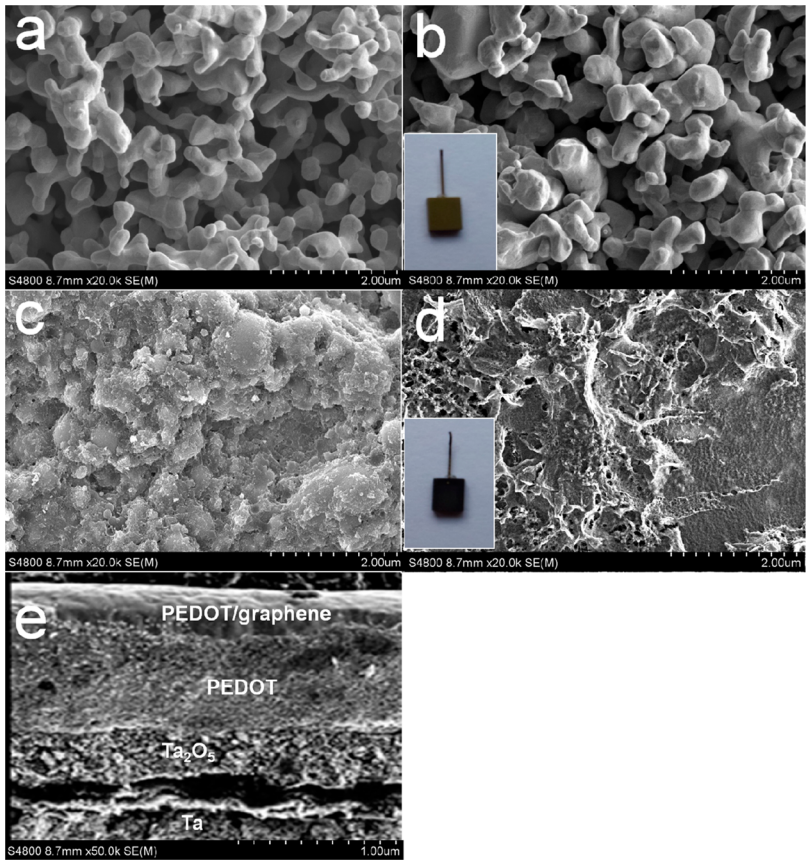

Figure 2. SEM images of (a) the high specific surface area sinter anode tantalum body, (b) Ta_2O_5 covered anode, (c) PEDOT covered tantalum body, (d) PEDOT/graphene covered tantalum body, and (e) the fracture structure of Ta/Ta_2O_5/PEDOT/graphene.

(SEM, Model S-2400). The conductivity of VPP PEDOT and PEDOT/graphene was characterized by a homemade four-point probe instrument. The capacitance, dissipation factor (DF), and equivalent series resistance (ESR) of capacitors were measured by the use of an HP 4263A LCR meter. The leakage current (LC) was measured by the use of the Tonghui LC testing instrument, model TH4321.

3. RESULTS AND DISCUSSION

One key issue in manufacturing anode vacuum sintered based solid tantalum electrolyte capacitors is to build up a robust cathode layer to protect the dielectric layer from possible mechanical damage. We figured out that the drawback of the Ta/Ta_2O_5/PEDOT capacitors using the VPP process is the fragility of the parts due to the powdery nature of chemically synthesized PEDOT. In order to overcome this problem, we develop a VPP PEDOT/graphene outer layer to improve the mechanical strength ability of the whole cathode film. This PEDOT/graphene outer layer not only improves the mechanical strength ability of the whole cathode but also reduces the cathode resistance due to the high conductive ability of graphene. The PEDOT/graphene may also result in lower contact resistance between PEDOT/graphene and the latter formed carbon paste due to suitable conductive ability and can further reduce the capacitor ESR effectively.

Figure 1 shows the typical two-step VPP procedure for the fabrication of PEDOT as well as PEDOT/graphene composites. The dip-coating oxidant and oxidant/graphene films produce a yellow color typical of FeTos. After exposure of FeTos and FeTos/graphene films in EDOT vapor, the film color of FeTos also changes from yellow to a deep violet corresponding to doping state of PEDOT. Figure 2a shows a typical sintered anode Ta porous structure, and the obtained high specific surface facilitates the fabrication of a large capacitance capacitor. Figure 2b exhibits a porous sintered anode body covered by a continuous tantalum pentoxide dielectric layer. The extremely porous nature of the pellet structure demands that some type of liquid or vapor preparation process is used to prepare the cathode plate. These processes of penetration into the depths of the structure facilitate the deposition of cathode films on the pore structure. The entire surface area of the dielectric Ta_2O_5 is fully covered with cathode film. To achieve full capacitance, it is indispensable that the whole dielectric layer is covered with the solid electrolyte (PEDOT in this work). As little dipping as possible and increasing speed for sintered anode body in and out of the FeTos solution are critical to achieve full capacitance extraction. A complete coverage of FeTos films on tantalum pentoxide surface is obtained by the use of this method. After the exposure of FeTos and FeTos/graphene covered anode body in EDOT vapor, the color of anode body changes from yellow (as shown in Figure 2b) to deep violet (as shown in Figure 2d) corresponding to polymerization of EDOT into PEDOT. Sufficient time for polymerization is required for this VPP process because of the low EDOT vapor pressure in the reactor. Enough time is needed for EDOT vapor to pervade into the films and adsorb on the oxidant spot. At least 30−60 min or a shorter time at higher temperature is needed to complete EDOT polymerization under ambient temperature. Figure 2c shows a close package of VPP PEDOT on tantalum pentoxide. It also exhibits particle morphology due to coverage

of an ultrathin PEDOT layer. After the VPP deposition of PEDOT/graphene, the particle disappears and the entire tantalum pentoxide surface is covered by PEDOT/PEDOT-graphene films (as shown in Figure 2d). Figure 2e presents the layers of Ta/Ta_2O_5/VPP PEDOT-graphene. The close contact of different layers demonstrates PEDOT/graphene is well adhered on Ta_2O_5, and excellent mechanical strength performance is realized. Due to the large size of the graphene sheet, the FeTos/graphene is not introduced as the inner layer to avoid the blockage of graphene to the pore structure. The blockage of pore structure leads to incomplete coverage of PEDOT/graphene on Ta_2O_5 as well as incomplete capacitance extraction. This effect is more conspicuous inside the Ta_2O_5 surface of porous structure.

Owing to the self-assembly of EDOT in crystalline FeTos films on the template, the VPP PEDOT films deposited on Ta_2O_5 exhibit a better uniform molecular structure. As shown in Figure 3, the XRD analysis presents the evidence of

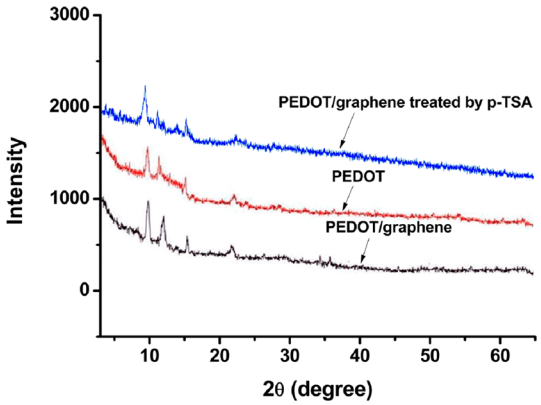

Figure 3. XRD analysis of VPP PEDOT/graphene, PEDOT, and PEDOT graphene treated by p-TSA deposited on sintered tantalum anode body.

diffraction peaks at 2θ = 10.8°, 12.3°, 16.5°, and 23.7°. These peaks are attributed to the crystalline lattice of PEDOT chains doped by tosylate anions. The XRD spectrum of PEDOT/graphene (and PEDOT/graphene treated by p-TSA) almost exhibits similar diffraction peaks but relative weak peak intensity. The close package of PEDOT on graphene results in the formation of crystalline PEDOT structure in nanocomposites.

To confirm the complete coverage of PEDOT on dielectric layer, enough time is needed for the VPP deposition of PEDOT films on tantalum pentoxide. As shown in Figure 4, the capacitance increases with the time used for polymerization. As a result of homogeneous PEDOT coating inside the tantalum oxide pores, the PEDOT/PEDOT-graphene device indicates satisfactory capacitance extraction at 1 h. However, the PEDOT-graphene device exhibits inferior capacitance extraction performance. As mentioned above, due to the larger size of graphene, the FeTos/graphene solution may block the pore structure and prevent the latter oxidant solution from forming a complete coverage inside tantalum pentoxide.

The conductivity is measured by the use of the four probe method. The obtained conductivities of as-prepared VPP PEDOT and PEDOT/graphene deposited on SiO_2 substrate are 160 ± 20 and 220 ± 20 s/cm, respectively. The conductivity of as-prepared VPP PEDOT/PEDOT-graphene nanocomposite is 200 ± 20 s/cm. The conductivity of pure

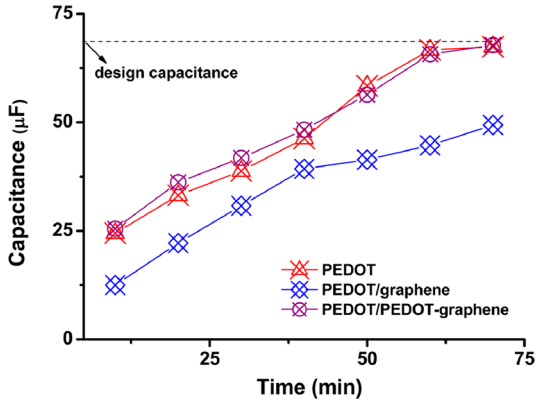

Figure 4. Capacitance extraction of capacitor on polymerization time of the VPP process.

VPP PEDOT is lower than that of the nanocompsite. Moreover, in order to make the conductivity of VPP PEDOT/graphene higher, the as-prepared PEDOT/PEDOT-graphene is treated by the use of *p*-toluenesulfonic acid (p-TSA). The as-prepared VPP PEDOT/PEDOT-graphene nanocompostie shows conductivity of 280 ± 20 s/cm after the p-TSA treatment. This enhanced conductivity is ascribed to the further doping of PEDOT by p-TSA. This is confirmed by UV−vis-NIR and FT-IR spectrum analysis (as shown in Figure 5).

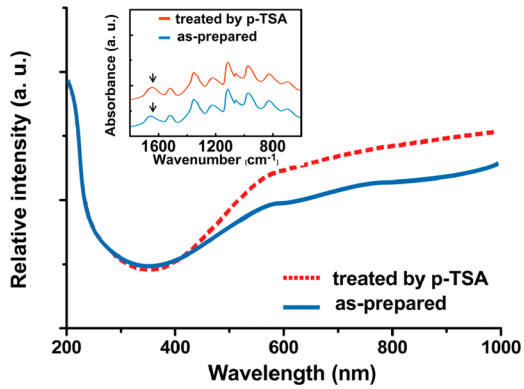

Figure 5. UV−vis-NIR and FT-IR spectrum of as-prepared PEDOT/PEDOT-graphene before and after the p-TSA treatment.

VPP PEDOT/PEDOT-graphene films indicate low absorption in the visible region. The absorption increases from 600 nm to the NIR (near-infrared) region ascribed to the increasing quantity of polarons and bipolarons attributed to partial doping of Tos in PEDOT during the polymerization process. Moreover, the FT-IR also reveals that the p-TSA treatment causes the further doping state of PEDOT. The absorption peak at 1640 cm^{-1} (noted by the arrow) reveals the PEDOT film has been doped after vapor phase polymerization. After being treated with p-TSA, the higher doping state of PEDOT, the higher intensity peak is observed at 1640 cm^{-1}. Furthermore, the peak shifts to higher wavenumber position (noted by the arrow).

The higher conductivity results in both resistance of cathode films and lower ESR of capacitors. Figure 6 shows the ESR-frequency characteristic of capacitors with different VPP cathode films. The PEDOT/PEDOT-graphene based capacitor exhibits ultralow ESR at about 12 mΩ and excellent ESR-

dx.doi.org/10.1021/am4003815 | ACS Appl. Mater. Interfaces 2013, 5, 4350−4355

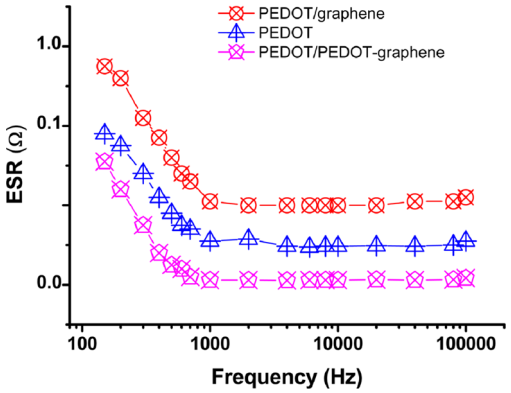

Figure 6. ESR versus frequency performance of tantalum capacitor with different VPP films as cathode films.

frequency performance. Although the PEDOT-graphene films exhibit high conductivity, the capacitor using pure PEDOT-graphene as cathode film shows high ESR. The results demonstrate that graphene blocks the pore structure during FeTos/graphene dip-coating. The latter FeTos/graphene solution can not penetrate into the depths of the pore structure to facilitate the deposition of PEDOT onto the inside of Ta_2O_5. Incomplete coverage of PEDOT on Ta_2O_5 leads to the enhancement of contact resistance between dielectric layer and carbon paste as well as the ESR of the capacitor.

The lower ESR of the tantalum capacitor makes the device exhibit an excellent capacitance-frequency characteristic. The tantalum electrolyte capacitor fabricated on sintered porous structure is similar to abundant particle capacitors with a parallel connection structure (as shown in Figure 1b). There is an additional resistance added to the capacitor element from its location to the termination points of the capacitor. With the increase of working frequency, the capacitance of deep particle capacitor declines, leading to a "roll-off" effect of capacitance. As shown in Figure 7, all capacitors made with VPP films show

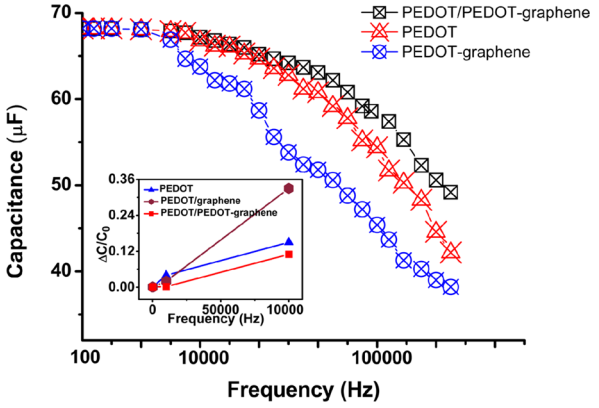

Figure 7. Capacitance versus frequency performance of different VPP film based tantalum capacitors, and the inset image shows capacitance change with the varying of frequency.

decaying capacitance as the frequency increases. The higher ESR accelerates the degeneration of capacitance. The PEDOT/PEDOT-graphene based capacitor exhibits excellent capacitance-frequency performance as it can keep 82% of initial capacitance at 500 kHz. The higher ESR of capacitor based on PEDOT-graphene displays a serious degeneration of capacitance as the frequency increases. The capacitance declines by 50% when the frequency is at 500 kHz. Compared with PEDOT/PEDOT-graphene, the inset image in Figure 7 also demonstrates the distinct capacitance change ($\Delta C/C_0$, C_0 is initial capacitance) that occurs in capacitors based on PEDOT and PEDOT/graphene due to the high ESR of these devices. These results indicate that the PEDOT/PEDOT-graphene nanocomposite layer fabricated on Ta_2O_5 is suitable for the use of cathode films as ultralow ESR tantalum capacitors.

As a practical electrical application, the tantalum electrolyte capacitors need to be encapsulated. The encapsulation process causes a mechanical force on entire capacitor body and anode Ta_2O_5 films, resulting in the degradation of leakage current in devices. In this work, the introduced PEDOT/graphene into cathode films not only improves the conductive ability of cathode films but also enhances the mechanical strength of cathode films. It prevents the cathode film from possible mechanical force damage. Figure 8 shows the comparison of

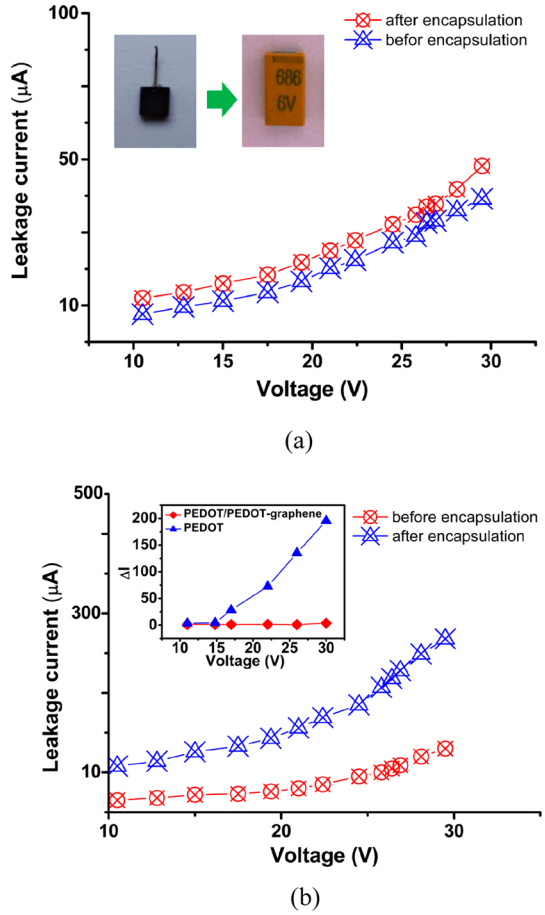

Figure 8. Influence of the device encapsulation process on leakage current of VPP (a) PEDOT/PEDOT-graphene film and PEDOT film based capacitors (b). The inset image in (b) shows the leakage current change (ΔI) of both capacitors, varying the applied voltage.

leakage current performance of capacitors based on VPP films. As shown in Figure 8a, the encapsulation process does not affect the leakage current of capacitor based on PEDOT/PEDOT-graphene, indicating the excellent mechanical strength of PEDOT/PEDOT-graphene to protect Ta_2O_5 dielectric layer. However, an obvious leakage current increment is observed in capacitors based on VPP PEDOT (as shown in Figure 8b). The fragile nature of PEDOT makes it unable to form an effective

dx.doi.org/10.1021/am4003815 | ACS Appl. Mater. Interfaces 2013, 5, 4350−4355

buffer layer to absorb or reduce the mechanical force during the encapsulation, causing mechanical destruction of Ta_2O_5 and the increase of leakage current. Compared with a capacitor based on PEDOT/PEDOT-graphene, the image in Figure 8b also shows the capacitor based on PEDOT exhibits a distinct increase of leakage current as the applied voltage increases. In addition, the effect of the encapsulation process on the other parameters of capacitors based on PEDOT/PEDOT-graphene is not observed. This capacitor shows stable electrical performance for practical electronic applications.

4. CONCLUSIONS

PEDOT/PEDOT-graphene nanocomposite films are prepared for use as cathode films for a solid tantalum electrolyte capacitor. The PEDOT inner layer and PEDOT-graphene outer layer are constructed on a porous Ta_2O_5 anode surface by the use of the VPP process. The incorporation of graphene into PEDOT results in improvement of conductivity and mechanical strength cathode film of capacitors. The high conductivity of PEDOT-graphene also resulted in lower contact resistance between PEDOT and carbon paste. The tantalum capacitor based on VPP PEDOT/PEDOT-graphene shows ultralow ESR, ca. 12 mΩ, and exhibits excellent capacitance vs frequency characteristics. The device encapsulation process does not affect the leakage current of the capacitor based on PEDOT/PEDOT-graphene, indicating that the excellent mechanical strength of PEDOT/PEDOT-graphene protects the Ta_2O_5 dielectric film from being destroyed during encapsulation. In conclusion, this highly conductive and mechanical strength graphene based polymer film shows a promising future for use as a high performance electrode material of capacitors, organic solar cells, and energy storage devices.

AUTHOR INFORMATION

Corresponding Author

*E-mail: shibinli@uestc.edu.cn. Tel: +86-28-83208959. Fax: +86-28-83206123.

Notes

The authors declare no competing financial interest.

ACKNOWLEDGMENTS

The work was supported by the National Science Foundation of China (NSFC) (No. 61101029 and No. 61204098),the Fundamental Research Funds for the Central Universities (No. ZYGX2010J057), and A Plan for Supporting the New Century Talents (No. NCET-12-0091).

REFERENCES

(1) Heeger, A. J. *Angew. Chem., Int. Ed.* **2001**, *40*, 2591−2611.
(2) Tanrıverdi, E. E.; Uzumcu, A. T.; Kavas, H.; Demir, A.; Baykal, A. *Nano-Micro Lett.* **2011**, *3*, 99−107.
(3) Guenes, S.; Neugebauer, H.; Sariciftci, N. S. *Chem. Rev.* **2007**, *107*, 1324−1338.
(4) Chronakis, I. S.; Grapenson, S.; Jakob, A. *Polymer* **2006**, *47*, 1597−1603.
(5) Khomenko, V.; Frackowiak, E.; Béguin, F. F. *Electrochim. Acta* **2005**, *50*, 2499−2560.
(6) Graeme, A.; Snook, P. K.; Adam, S. B. *J. Power Sources* **2011**, *196*, 1−12.
(7) Gerhard, H. W.; Friedrich, J. *Adv. Mater.* **2004**, *4*, 116−123.
(8) Kudoh, Y.; Akami, K.; Matsuya, Y. *Synth. Met.* **1999**, *102*, 973−974.
(9) Ci, L.; Suhr, J.; Pushparaj, V.; Zhang, X.; Ajayan, P. M. *Nano Lett.* **2008**, *8*, 2762−2766.
(10) Kelly, T. L.; Yano, K.; Wolf, M. O. *ACS Appl. Mater. Interfaces* **2009**, *1*, 2536−2543.
(11) Fichet, O.; Francois, T. V.; Dominique, T.; Chevrot, C. *Thin Solid Films* **2002**, *411*, 280−288.
(12) Jung, M. H.; Lee, H. Y. *Langmuir* **2008**, *24*, 9825−9831.
(13) Wang, Y.; Tran, H. D.; Kaner, R. B. *J. Phys. Chem. C* **2009**, *113*, 10346−10349.
(14) Tenhaeff, W. E.; Gleason, K. K. *Adv. Funct. Mater.* **2008**, *18*, 979−992.
(15) Acqua, L. D.; Tonina, C.; Varesanoa, A.; Canettib, M.; Porziob, W.; Catellani, M. *Synth. Met.* **2006**, *156*, 379−386.
(16) Sreenivasan, R.; Gleason, K. K. *Chem. Vap. Deposition* **2009**, *15*, 77−90.
(17) Jensen, B. W.; Chen, J.; West, K.; Wallace, G. *Macromolecules* **2004**, *37*, 5930−5935.
(18) Tenhaeff, W. E.; Gleason, K. K. *Adv. Funct. Mater.* **2008**, *18*, 979−992.
(19) Jensen, B. W.; West, K. *Macromolecules* **2004**, *37*, 4538−4543.
(20) Kim, J. Y.; Kwon, M. H.; Min, Y. K.; Kwon, S.; Ihm, D. W. *Adv. Mater.* **2007**, *19*, 3501−3506.
(21) Madl, C. M.; Kariuki, P. N.; Gendron, J.; Piper, L. F. J.; Jones, W. E., Jr. *Synth. Met.* **2011**, *161*, 1159−1165.
(22) Han, Y.-H.; Sejdic, T. J.; Wright, B.; Yim, J.-H. *Macromol. Chem. Phys.* **2011**, *212*, 521−530.